J. Great Lakes Res. 34:36–53
Internat. Assoc. Great Lakes Res., 2008

Large-scale 700 hPa Height Patterns Associated with Cyclone Passage and Strong Winds on Lake Erie

Brent M. Lofgren[1,*] and Peter Bieniek[2,†]

[1]*NOAA/Great Lakes Environmental Research Laboratory*
2205 Commonwealth Blvd.
Ann Arbor, Michigan 48105

[2]*Cooperative Institute for Limnology and Ecosystems Research*
University of Michigan
Ann Arbor, Michigan 48109

ABSTRACT. *The difference in 700 hPa height patterns was examined on a seasonal basis between years with high numbers and low numbers of cyclone passages through Lake Erie, and high and low numbers of strong wind events at Cleveland Hopkins Airport. These show that both cyclones and strong wind events often are associated with atmospheric patterns resembling the negative phase of the North Atlantic Oscillation, or the negative phase of the Arctic Oscillation. Custom teleconnection indices were derived from these maps of 700 hPa height differences, and the seasonal means of each of these indices were linearly regressed against the number of cyclones and the number of strong wind events in that season for each year. This procedure led to moderate, but statistically significant, correlation coefficients. This gives some basis for probabilistic prediction of cyclone passages and strong wind events at Lake Erie. Actual application in prediction will require skill also in predicting the geopotential heights, and predictions generalized over larger areas may have greater significance and robustness.*

INDEX WORDS: *Lake Erie, strong wind events, high wind events, teleconnections, cyclones.*

INTRODUCTION

According to the geostrophic relation, strong winds can result from strong pressure gradients, which often occur in the vicinity of low pressure centers. However, they can also result from mesoscale events such as convective precipitation events and thunderstorms. Strong wind events drive episodic evaporation from lakes (Blanken *et al*. 2003) and can also drive forced turbulence within lakes, with consequences for vertical mixing of nutrients and resultant biological effects (Lam and Schertzer 1987). They can also affect the formation and transport of ice. Hence, as an adjunct to the Great Lakes Environmental Research Laboratory's (GLERL) International Field Year for Lake Erie (IFYLE, Hawley *et al.* 2006), we have sought to investigate the occurrence and characteristics of both low pressure systems and strong wind events on Lake Erie based on some continental- or hemispheric-scale atmospheric patterns. The low pressure systems will be referred to here as "cyclones."

Grover and Sousounis (2002) carried out an intensive analysis of synoptic-scale weather patterns, their association with precipitation at a station in Grand Rapids, Michigan, and their relation to some hemispheric-scale atmospheric patterns, concentrating on the fall season. They found that fall precipitation has increased over the past 60 years mainly through events associated with warm, stationary, and occluded fronts, with a trend toward their supplanting cold front and low pressure situations as the dominant precipitation-generating patterns. While all of these types of fronts (warm, stationary, occluded, and cold) tend to occur in complexes including a low pressure center, the portion of the system that was closest to the point of interest was used for classification purposes by Grover and Sousounis (2002). Greater precipitation was also associated with more zonal 500 hPa flow, a stronger subtropical jet in upper levels, increased moisture

*Corresponding author. E-mail: Brent.Lofgren@noaa.gov
†Current affiliation: Geophysical Institute, University of Alaska, P.O. Box 751503, Fairbanks, AK 99775

and low-level baroclinicity, and stronger low-level southerly flow.

Other studies have looked more broadly at the passage of low pressure complexes through the Great Lakes region and the statistical association of this with larger-scale patterns. Isard *et al*. (2000) analyzed the incidence of cyclone passage within a large area surrounding the Great Lakes, and found a greater incidence of cyclones in the region during times of negative Pacific-North America (PNA) index than during time of positive PNA index. This applies particularly to cyclones originating from the west and southwest. The PNA is a pattern of geopotential heights, often defined at 500 hPa, but also at 700 hPa, that in the positive phase has a train of high geopotential height near the equator in the Pacific, low in the northern Pacific, high over northwestern North America, and low over southeastern North America (Wallace and Gutzler 1981, Barnston and Livezey 1987).

Rodionov (1994) found additional correlations with precipitation. Wintertime precipitation over the Great Lakes basin is strongly correlated to an index of 700 hPa height (his equation 4) that he calls the Great Lakes (GL) index. The GL index is related to the PNA pattern, but has its centers of action somewhat shifted in space in order to optimize its correlation to Great Lakes precipitation. Although Rodionov (1994), in his Figure 4, shows a center of action in the North Atlantic near Iceland, reminiscent of the North Atlantic Oscillation (NAO), this center of action is not included in the discussion.

The NAO is a pattern defined by either mean sea level pressure or by 700 hPa height, in which the positive phase of the NAO has anomalously low pressure/geopotential height over the Atlantic sector in the vicinity of 60° N latitude and anomalously high pressure/geopotential height over the Atlantic near 40° N, thus enhancing the ambient pattern of Azores High and Icelandic Low (Barnston and Livezey 1987). The negative phase has the opposite anomalies. The Arctic Oscillation (AO) is a pattern that is related to the NAO, but with pressure anomalies that spread beyond the North Atlantic sector to cover much of the northern continents of the Northern hemisphere along with the Arctic Ocean as one end of the dipole, and the midlatitude parts of the continents as well as the oceans as the other part of the dipole.

Rodionov (1994) demonstrates that one can create custom indices that may be well-correlated with climatic variables in a particular area of interest, and while they may not correspond to one particular standard teleconnection pattern, a combination of patterns, such as both PNA and NAO, may correspond more closely to the correlated pattern and may facilitate some predictive skill. These combinations of teleconnections may be the cause of changes in average jet stream position and strength over seasonal periods, although the causality could also potentially be reversed—latitudinal mixing of air resulting from cyclone activity can affect the thermal gradient over the North Atlantic that results in a general pattern of northern high pressure and southern low pressure.

Although the preceding discussion shows that attention has been paid to the connection of cyclones and frontal weather systems to precipitation events, and of teleconnection indices to seasonal precipitation, there seems to be little parallel work on wind events. In this paper, we attempt to find connections (1) between wind events and the passage of cyclones, and (2) seasonal-to-annual incidence of cyclone passage and custom-defined teleconnection indices that optimize correlation with these events. This is carried out specifically in the context of Lake Erie.

DATA

The dataset of Serreze *et al.* (1997) is used for tracking cyclones through the region of Lake Erie. This dataset is derived from the NCEP/NCAR Reanalysis Dataset (Kalnay *et al*. 1996), which has a grid spacing of 2.5 degrees. With such a coarse spacing, there are only two grid points in the immediate vicinity of Lake Erie, one at 42.5° N, 80° W, in the eastern part of Lake Erie, and one at 42.5° N, 82.5° W, just north of the western part of Lake Erie. Serreze *et al*. (1997) define a cyclone as a grid point surrounded by grid points with sea level pressure at least 2 hPa higher. Their tracking algorithm usually involves locating a cyclone in the same or adjacent grid points at successive 12-hour reporting intervals; some more involved rules are occasionally invoked when a cyclone might have traveled a greater distance during that time. We use both the Serreze *et al.* (1997) and Kalnay *et al.* (1996) data between 1951 and 2003.

Wind data were acquired from the edited historical wind data available from the National Climatic Data Center for stations at Cleveland Hopkins Airport (41.4° N, 81.85° W). In order to compensate for the changes with time in anemometer height at this station, a correction was made to the measured

wind speeds, following Peterson and Hennessey (1978): $v_c = v_a(10\ \text{m}/h_a)^{0.14}$, where v_c is the estimated wind speed at 10 m height, v_a is the wind speed measured by the anemometer, and h_a is the height of the anemometer above the surface at the station.

METHODS

A variety of teleconnection indices are recognized, but in this study we have chosen to define custom indices that might best predict cyclone passages and number of strong wind events on a seasonal basis for the Lake Erie region.

We used the cyclone path dataset of Serreze *et al.* (1997) to get the number of distinct cyclones passing through the Lake Erie grid points (42.5° N, 80° W and 42.5° N, 82.5° W) during each of the standard meteorological seasons for each year: December-January-February (DJF, with the December being from the year previous to the year used for labeling the season), March-April-May (MAM), June-July-August (JJA), and September-October-November (SON). There are 53 years (1951–2003) for which we analyzed both the Serreze *et al.* (1997) data and the NCEP-NCAR reanalysis data, and we tried to choose the ten years with the greatest number of cyclone passages and the 10 years with the smallest number. Because of the discrete numbers of cyclone passages, ties are frequent, and subjective decisions were made to get numbers of years near ten, with years tied with one another for number of cyclones all either included or excluded.

Difference maps were made for 700 hPa heights by subtracting the values for the years with the smallest number of cyclone passages from those for the years with the greatest number, in each season. From these maps, centers of low and high values of difference in geopotential height were chosen in order to define custom indices by which the number of cyclone passages can be linked to the geopotential height patterns. The selection of centers involved some subjective choice, with the greatest magnitude of positive and negative height differences generally being chosen, but with preference being given to centers located over or near the North American continent. The statistical significance of these high and low centers was also given consideration in choosing the definition of the custom index, and for a few seasons, alternative indices are presented here.

The seasonal mean value of these custom indices was then calculated for each year, and correlated with the number of cyclones during that season. We did not anticipate any theoretical reasons or find any empirical evidence to argue for using a regression method other than a simple linear regression between atmospheric indices and number of cyclones. One difficulty is that the numbers of cyclones are always integers, while the indices are values along a continuum.

In order to get more directly at wind events, this procedure was repeated using strong wind events rather than cyclone passages. Starting from hourly values of wind speed at the stations, adjusted for anemometer height as described in section 2, the daily maximum wind was derived. A cutoff value was established that included all events that tied or exceeded the value of the day at the 96th percentile for a season, and a count was made of all days within that season of each year on which that wind speed was met or exceeded. Although the adjustment for anemometer height produced some differentiation, many ties still occurred because wind speeds are reported in integral numbers of knots. Following this, the top and bottom years (roughly ten of each) were used to define a custom index, and correlations to this index were calculated.

RESULTS

Cyclone Track Climatology

The tracks of cyclones entering the Lake Erie area during the years 1980 to 2003, according to the data of Serreze *et al.* (1997), are shown in Figure 1. During DJF (Fig. 1a), there are more cyclones than in the other seasons, almost all coming from a direction with a westward component. Although Whittaker and Horn (1984) noted discrete tracks for cyclones entering the vicinity of the Laurentian Great Lakes, Figure 1a does not give strong evidence of separation among distinct tracks. Rather, it gives a range of directions of origin, from south-southwest to northwest, with a few exceptional tracks during this time period having the final stage of their approach from the south, south-southeast, and northeast.

During MAM (Fig. 1b) there are slightly fewer cyclones that reach Lake Erie, and considerably fewer during JJA (Fig. 1c). During these seasons, especially during JJA, the cyclones are generally of lesser intensity as well (not shown). During these seasons, they tend to originate from directions more directly to the west compared to DJF, although several tracks during MAM approach from the northwest and a small number from the northeast and

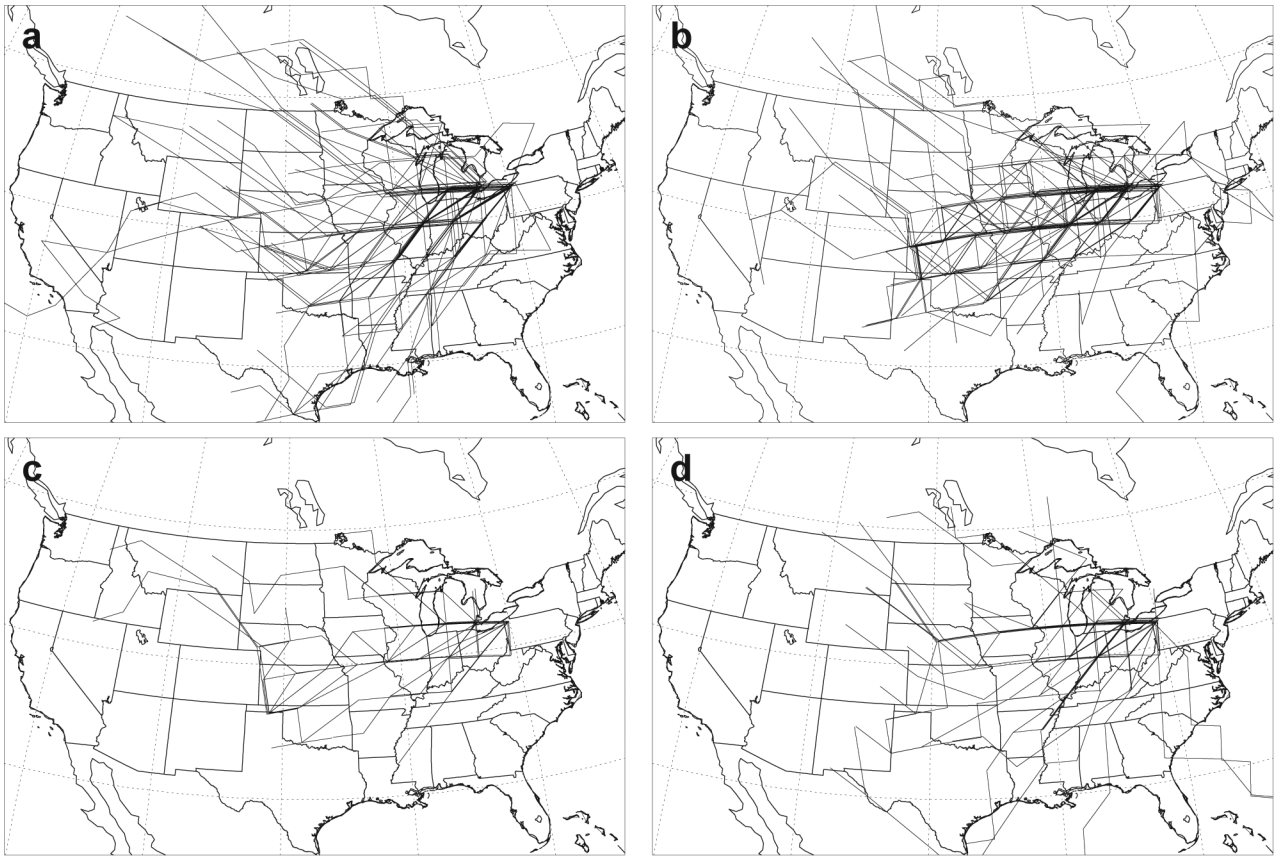

FIG. 1. Cyclone tracks for (a) December, January, and February; (b) March, April, and May; (c) June, July, and August; and (d) September, October, and November, using the tracks from the dataset of Serreze* et al. *(1997) that pass through the grid points corresponding to Lake Erie and tracing backward to their origin. For clarity of the figures, only the data from 1980 to 2003 are used. Because the cyclones are identified at discrete grid points, the tracks are spatially offset by a small amount in order to avoid direct overlap.

southeast. During SON (Fig. 1d), there are fewer tracks than during DJF and MAM, with several of them originating from the northwest and southwest.

Cyclone Frequency and Teleconnections

The presentation of results here will examine patterns of 700 hPa height correlated to cyclone passage over Lake Erie and strong wind events at Cleveland Hopkins airport. The patterns of difference in 700 hPa height between the most active years and the least active years in terms of cyclone passage are shown in Figure 2. The years used are shown in Table 1.

The 700 hPa height pattern associated with high numbers of cyclones over Lake Erie during DJF (Fig. 2a) shows a pattern similar to the negative phase of the NAO (with the distinction that the standard definition of the NAO uses mean sea level pressure rather than 700 hPa height) or, because of the broad longitudinal extent at high latitudes, the AO. The secondary positive center over northeastern North America in this case forms an extension of the broad high pressure anomaly at high latitudes.

A set of simple dipole indices was defined to attempt to capture a correlation with cyclone passages. The choice of points from which to construct dipole indices was subjective, with preference given for magnitude of the observed anomaly, proximity to the area of interest (Lake Erie), and statistical significance if possible. The index that was defined as a first guess for DJF was constructed by subtracting the geopotential height at 42.5° N, 20° W from that at 80° N, 55° E (Table 2). While the

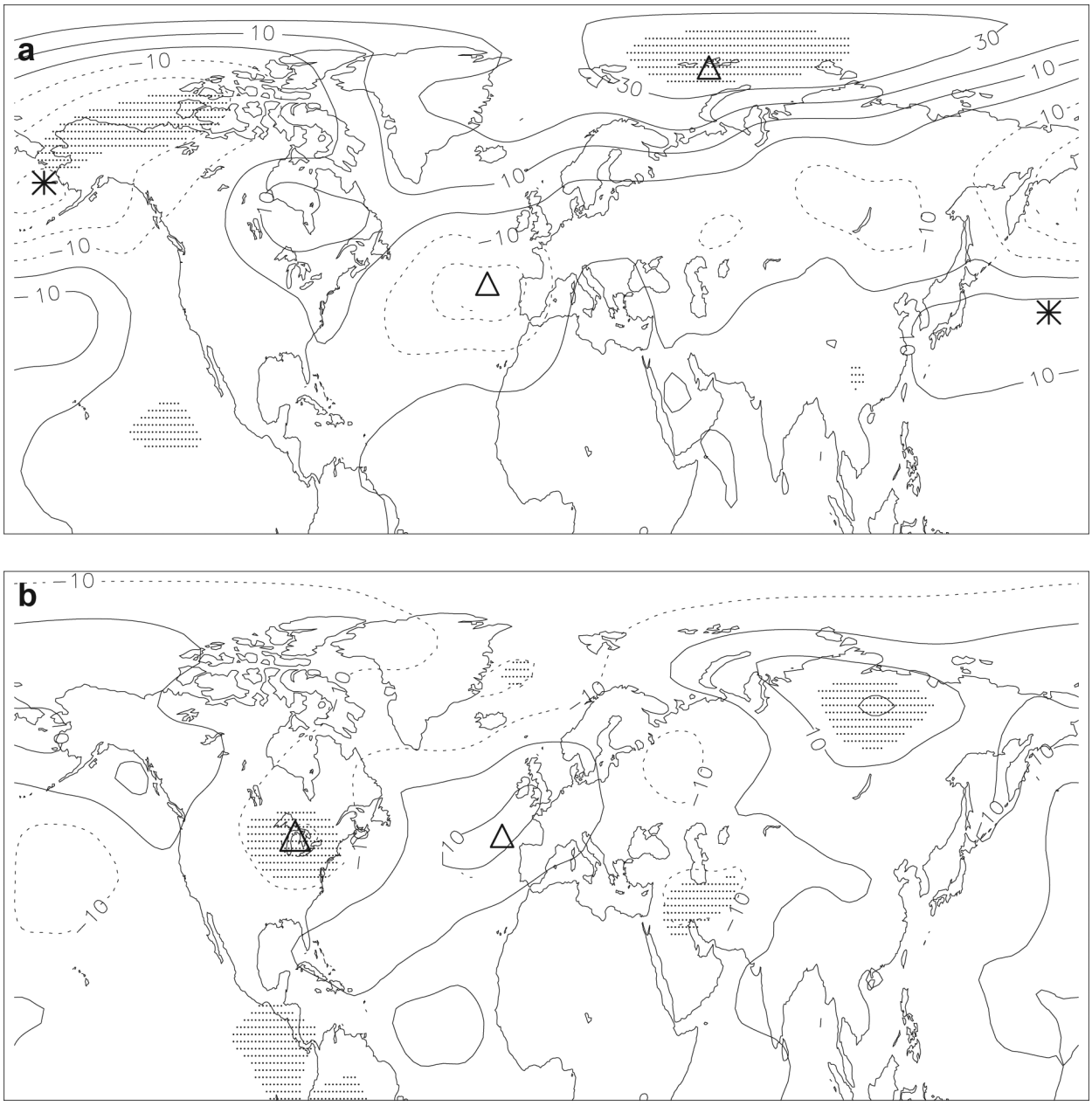

FIG. 2. Difference in 700 hPa height (m) between the years with high numbers of cyclone passages and those with low numbers of cyclone passages through the Lake Erie area (high years minus low years) during the seasons of (a) December, January, and February; (b) March, April, and May; (c) June, July, and August; and (d) September, October, and November. The shaded regions indicate statistical significance at the 95% level by a two-tailed Student's t-test. The years used for each of these seasons are given in Table 1. Triangles indicate the positive and negative centers of the custom indices defined in Table 2, while asterisks indicate the positive and negative centers of the "DJF Pacific" index and the "SON North America" index.

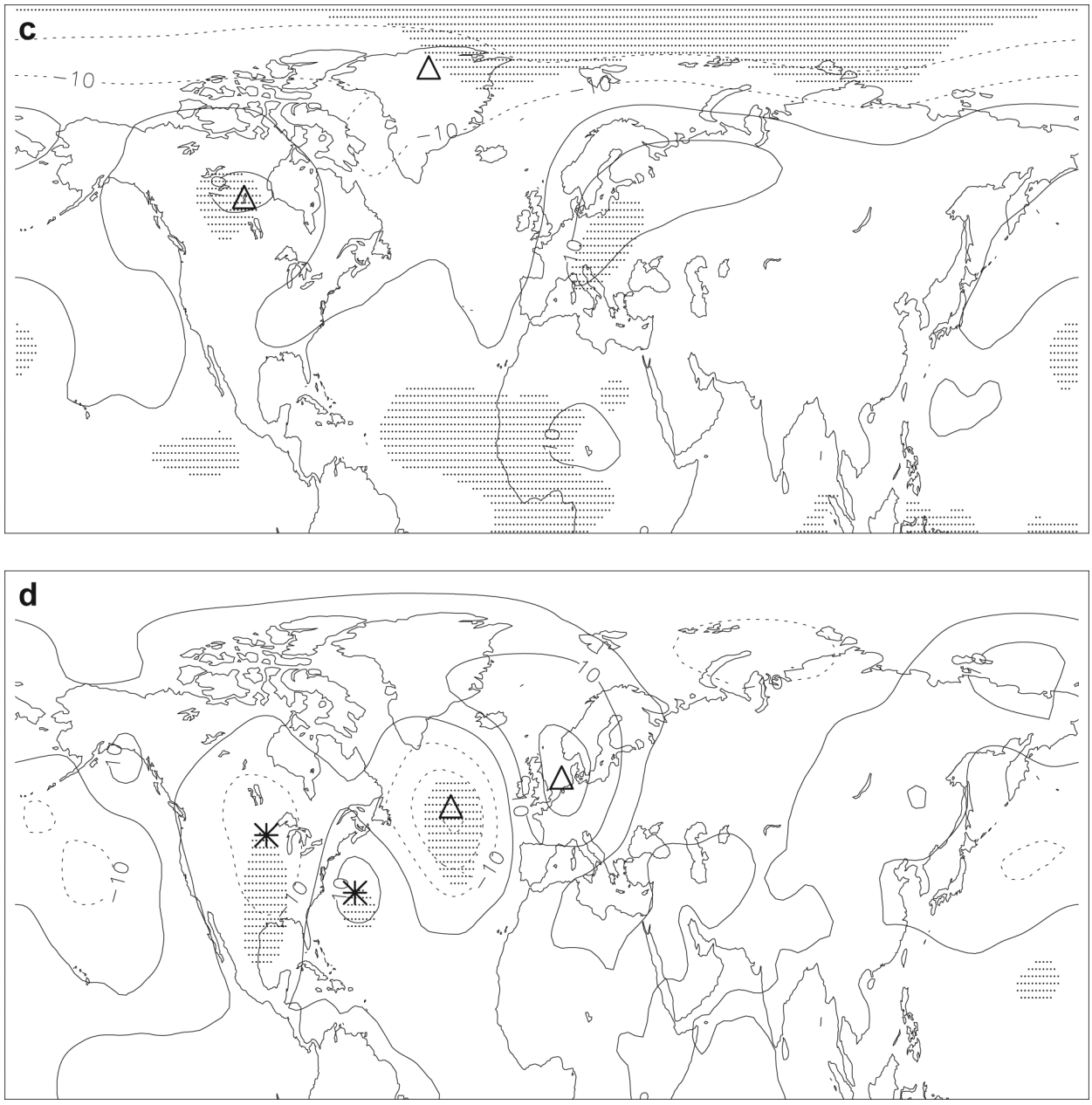

FIG. 2. Continued.

latter positive center shows statistical significance in Figure 2a, the former negative center does not. The scatterplot of number of cyclones per DJF season vs. this custom-defined index is shown in Figure 3a. The linear regression shown has an R^2 value of 0.047. We have a sample size of 53 years; for a 50-member sample set, the 0.05 level of likelihood for a one-tailed test is reached at $R^2 = 0.053$. Thus, we have not reached the 95% level of confidence that the slope of the regression line is greater than zero. Furthermore, the slope of the regression line is small, limiting its predictive capacity.

Although the passage of greater numbers of surface low pressure systems when the 700 hPa height is higher over the Great Lakes region seems counter-intuitive, these conditions are not entirely contradictory. Seasonal mean anomalies in pressure or geopotential height can produce only relatively small gradients relative to cyclones; cyclones are defined by the pressure relative to adjacent grid

TABLE 1. Years with high and low number of cyclone passages through the Lake Erie region during each season. The threshold number of cyclone passages required to be in each category is indicated in parentheses.

Season	Years with high number (minimum)	Years with low number (maximum)
December, January, February	1952, 1954, 1955, 1960, 1976, 1977, 1978, 1986, 1987, 1991, 1992, 1997, 1998, 2001 (6)	1961, 1962, 1963, 1971, 1981, 1983, 1989, 1994, 1995, 1996, 2003 (2)
March, April, May	1951, 1952, 1953, 1956, 1961, 1965, 1972, 1980, 1982, 1983, 1984, 1989, 1992, 1997 (6)	1958, 1962, 1976, 1977, 1985, 1987, 1993, 1996, 1999, 2000, 2001 (2)
June, July, August	1951, 1953, 1960, 1963, 1970, 1971, 1972, 1976, 1981, 1982, 1983, 1985, 1987, 1989, 1991, 1992, 1994 (3)	1954, 1955, 1957, 1958, 1959, 1961, 1962, 1965, 1966, 1969, 1974, 1975, 1977, 1978, 1979, 1984, 1990, 1993, 1995, 1999, 2000 (1)
September, October, November	1953, 1959, 1970, 1975, 1976, 1979, 1985, 1995, 2002 (4)	1956, 1963, 1964, 1965, 1969, 1974, 1991, 1998, 1999, 2000, 2003 (1)

points, not to larger field; and cyclone passages represent a higher moment of temporal variation than seasonal mean values.

However, the pattern of geopotential height differences shown in Figure 2a shows additional centers of anomalies in the Pacific Ocean region. Thus we define the index called "DJF Pacific" in Table 2. This pattern bears some resemblance to the Western Pacific pattern and the Pacific Decadal Oscillation, but has its southern (positive) center located too far north to match either of these. While there is not statistical significance shown in Figure 2a right at either of the points used to define this dipole, its negative center, defined at the point of greatest negative value, has a region of statistical significance to the northeast. This indicates that while the difference between the two groups of years that were used was not as great to the northeast of the negative center, the ambient interannual variability there is less, giving it a more significant *t* statistic. The regression to this index is shown in Figure 4a; it has a similar slope as Figure 3a, and its R^2 value is 0.067, thus exceeding the 95% confidence level. Still better correlation ($R^2 = 0.80$) is achieved by using the "DJF Arctic" index, which uses the two high-latitude centers shown in Figure 2a and named in Table 2. The scatterplot and regression for this index are in Figure 4b.

Finally for this season, we combined the two indices for DJF by addition and created the "DJF quadropole" index. This index sums the geopotential heights at 80° N, 55° E and 37.5° N, 170° E,

TABLE 2. Coordinates used in calculation of custom teleconnection indices for cyclone passages over Lake Erie during each season, as well as R2 values for the regressions shown in Figures 2 and 3. Indices are calculated by taking the geopotential heights at the coordinates labeled "positive center" minus those at the negative center, and subtracting the mean value over all years. Bold letters for the coordinates means that the 700 hPa geopotential height anomaly at that point, shown in Figure 2, is statistically significant at the 95% level of certainty. These points are indicated by triangles and asterisks in Figure 2.

Season	Positive center	Negative center	R^2
December, January, February	**80° N, 55° E**	42.5° N, 20° W	0.047
March, April, May	45° N, 15° W	**45° N, 85° W**	0.158
June, July, August	**57.5° N, 102.5° W**	**80° N, 40° W**	0.100
September, October, November	55° N, 5° E	**50° N, 32.5° W**	0.151
December, January, February Pacific	37.5° N, 170° E	60° N, 170° W	0.067
December, January, February Arctic	**80° N, 55° E**	60° N, 170° W	0.080
December, January, February quadrupole	**80° N, 55° E** 37.5° N, 170° E	42.5° N, 20° W 60° N, 170° W	0.106
September, October, November North America	**35° N, 65° W**	**45° N, 95° W**	0.223

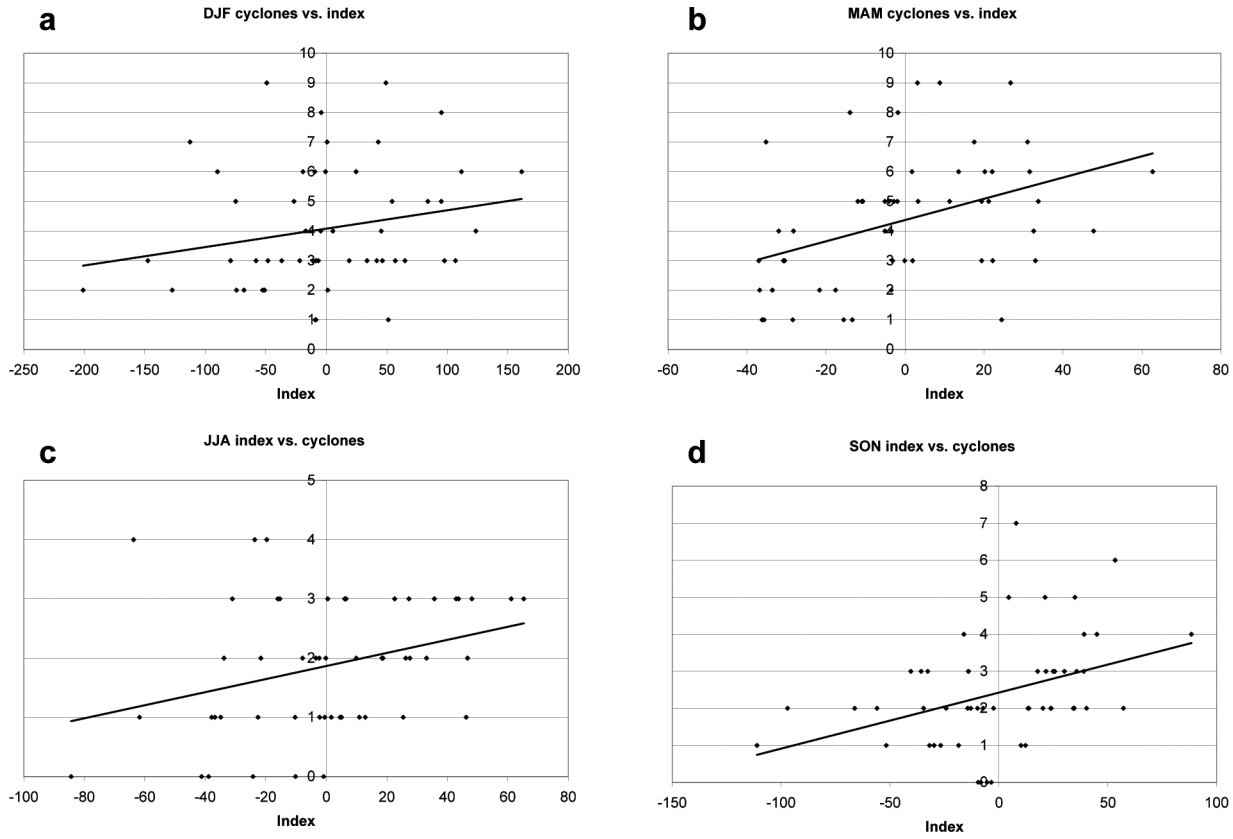

FIG. 3. Scatter plots of number of cyclones passing through the Lake Erie area vs. custom indices of 700 hPa height (m) designed to indicate frequency of cyclone passage, based on the patterns of 700 hPa height difference shown in Figure 2. Panels are (a) December, January, and February; (b) March, April, and May; (c) June, July, and August; and (d) September, October, and November. The definitions of the indices are shown in Table 2.

and subtracts the heights at 42.5° N, 20° W and 60° N, 170° W. This combination of the two dipole indices results in a greater R^2 of 0.106. As a simple indicator of the amount of information that can be derived from this regression, the regression line in Figure 4c, within the range of indices that have been observed, predicts a range of number of cyclones between 2.62 and 5.33, while the observed numbers range from 1 to 9. Thus, even if we consider this definition of the index to be optimal and can predict this index correctly, the resulting best-guess predictions will cover only about one-third of the observed range of values, and most of the variation will remain unpredictable.

During the MAM season, more cyclones occur when the 700 hPa height is high over the eastern Atlantic and low directly over the Laurentian Great Lakes (Fig. 2b). The magnitude of these centers is comparable to those found for DJF (Fig. 2a), and the correlation between the index and cyclones is better (R^2 = 0.158). However, the positive center off the west coast of Europe does not have significance at the 95% level.

The patterns in 700 hPa height differences between years with greater number of cyclones during JJA and those with lower numbers have smaller amplitude and broader spatial features (Fig. 2c). However, there are statistically significant centers of both positive and negative values in the North America-Arctic region. One factor at work here is the generally smaller number of cyclone passages during JJA, resulting in a larger number of years tied at each value. Seventeen years, each with three or four cyclones, are chosen as the high years, while 21 years, each with zero or one cyclone, are the low years (Table 1), excluding only the years with exactly two cyclones during JJA. The R^2 value for index-cyclone correlation during JJA is 0.100.

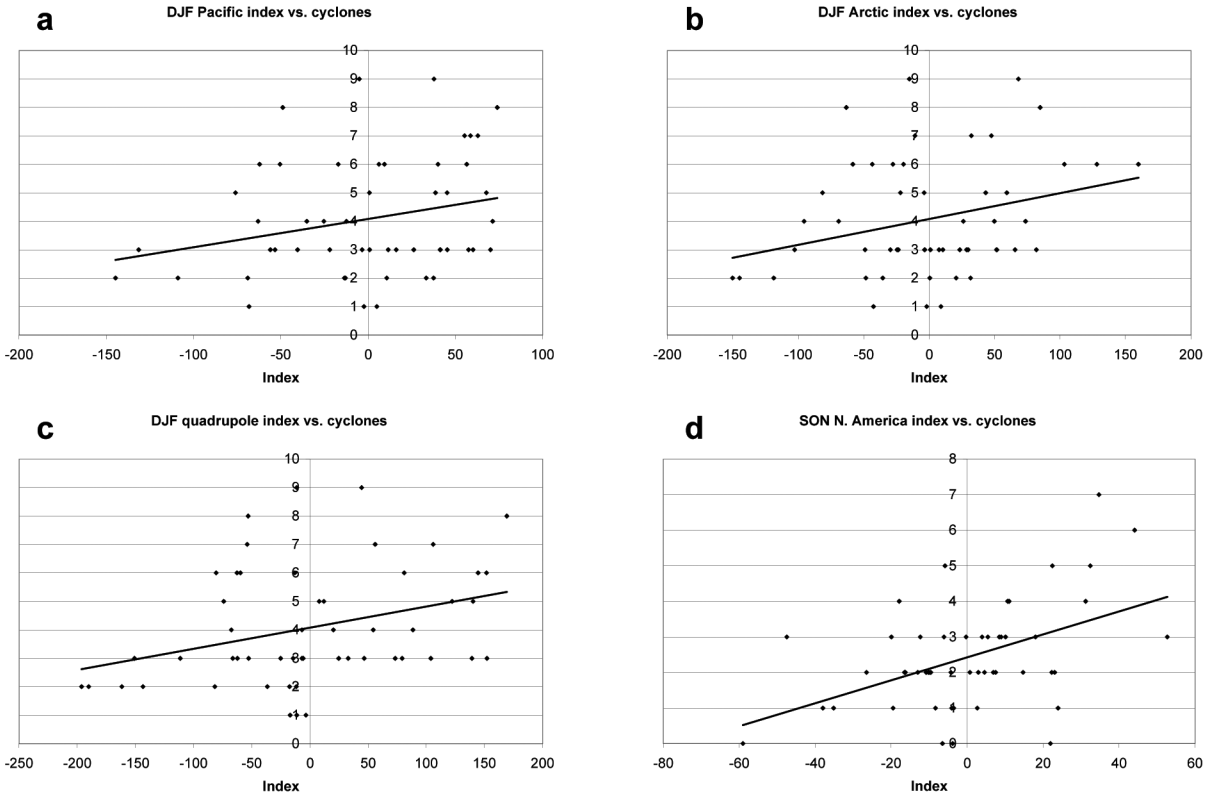

FIG. 4. As in Figure 3 but for (a) the December, January, February Pacific index; (b) the December, January, February Arctic index; (c) the December, January, February quadrupole index; and (d) the September, October, November North America index. The definitions of the indices are shown in Table 2.

Figure 2c also includes a sizable area of statistically significant 700 hPa height anomalies over western Africa and extending to the west, and similar regions will appear in later figures. These locations generally have small magnitude of height anomaly signal compared to locations at higher latitudes, but this is offset by small ambient variability to result in statistical significance. These distant regions of low signal are ignored for purposes of defining indices.

During SON, the greatest amplitude feature is a dipole between the North Sea region by northwestern Europe, and the north-central Atlantic (Fig. 2d). This dipole was used as a first guess but lacks statistical significance in the North Sea. The index defined using this correlates to cyclone passage during this season with an R^2 of 0.151.

Another index is also devised for the SON season, called the "SON North America" index (Table 2). Even though the magnitude of both centers of this index are less than those in the initial SON index, both of them are significant at the 95% level. The regression shown in Figure 4d has an R^2 of 0.223, and the linear fit ranges from about 0.5 cyclones to greater than 4, covering a large piece of the observed range from 0 to 7.

A simple resampling scheme was used to help verify the robustness of the patterns shown in Figure 2. Various years were dropped from the calculation, choosing the chronologically first half of those years that had a number of cyclone that tied with several others at the threshold value for the high range of cyclone number, along with the chronologically first half of the years that were tied at the threshold for the low range of cyclone number. These datasets were also matched with sets that excluded the last half of the years that were tied at the threshold of each group. Thus there were four pairs of datasets corresponding to each panel of Figure 2, each with the high cyclone group of years and low cyclone group reduced by 3 to 5 years. With the exception of the point near Greenland during JJA, centers of the respective low and high geopotential height were at

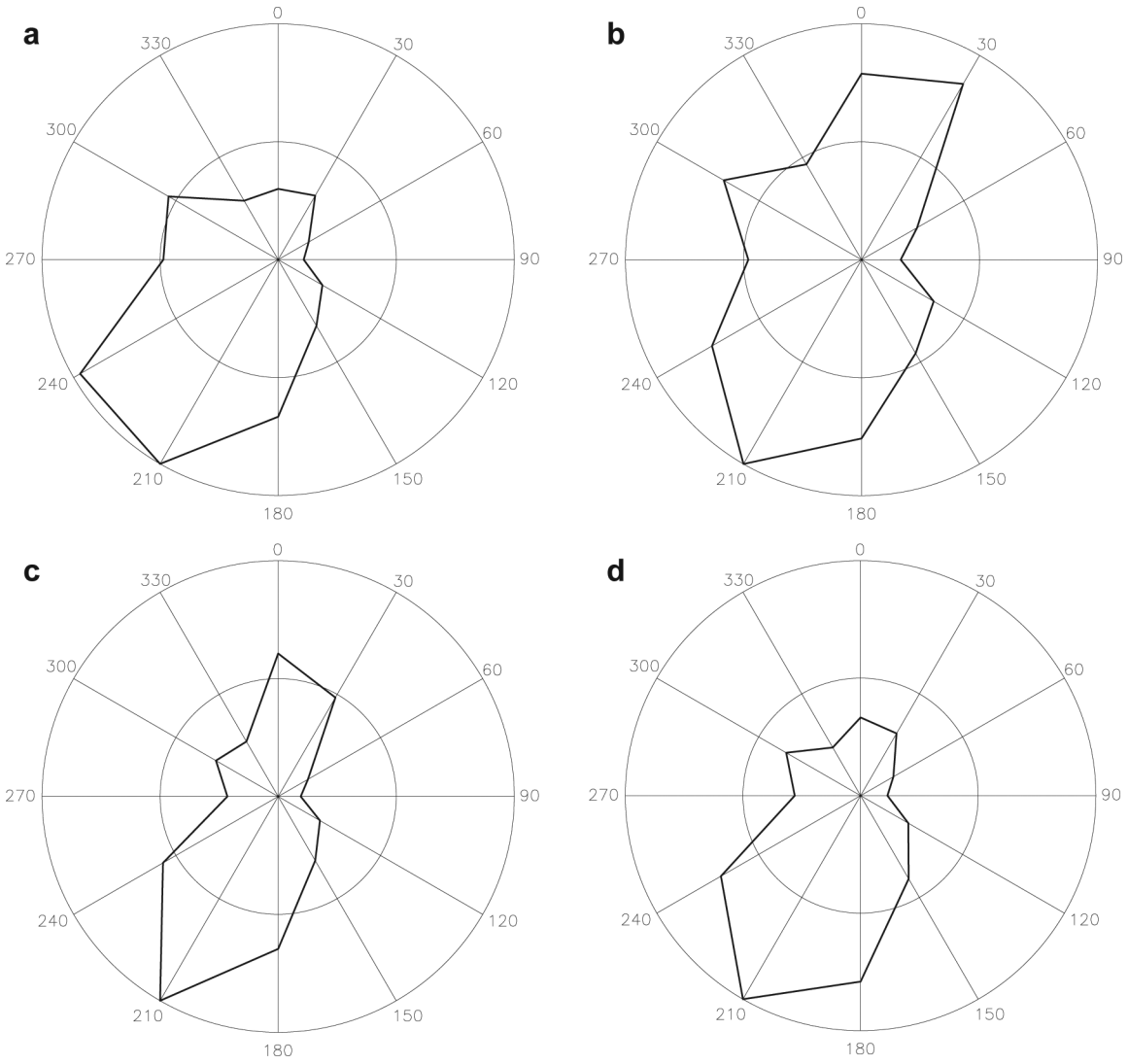

FIG. 5. Wind roses showing the frequency of various wind directions at Cleveland Hopkins Airport during (a) December, January, and February; (b) March, April, and May; (c) June, July, and August; and (d) September, October, and November. Winds are binned into 30° sectors and their frequencies are normalized so that the most frequent bin of wind direction corresponds to the outer circle of the wind rose.

or near those defined in Table 2 for all of these subsampled sets (not shown). As expected, the proximity of the low and high geopotential height centers in the subsampled sets was closer to that of the full set in cases where the statistical significance of the geopotential height anomaly was greater.

Wind Climatology in Cleveland

Many strong wind events are associated with cyclone passages, but in order to assess them more directly, a similar analysis is carried out keying on strong wind events in Cleveland rather than cyclones. In the wind readings from Cleveland Hopkins Airport, there is some seasonality to the wind speed and direction, but not a large amount. The wind direction (Fig. 5) is most frequently from the southwest in all seasons, with a secondary local maximum from the north and northeast, especially during MAM and JJA. While lake effects may have some influence on wind direction, winds that are predominantly from the south-southwest are not likely to be forced by a shoreline that is oriented

TABLE 3. Various percentile ranks of daily maximum wind speed (m/s) by season at Cleveland Hopkins Airport.

percentile	5	10	25	Median	75	90	95
DJF	4.65	5.45	6.71	8.16	10.08	11.67	13.41
MAM	4.80	5.76	6.61	7.77	10.08	11.62	13.45
JJA	4.32	4.80	5.76	6.72	8.05	9.60	10.28
SON	4.32	4.80	5.81	7.20	8.64	10.56	11.62

from the west-southwest to east-northeast, or in some nearby areas, directly west to east.

Daily maximum wind speeds are summarized in Table 3, with the values of various percentile ranks shown by season. The winds are strongest during the DJF and MAM seasons, with nearly identical values between these two seasons at all percentile levels. The values for the JJA and SON seasons are smaller than those for DJF and MAM by amounts ranging from 10% to 25%. While JJA and SON have identical values for the 5th and 10th percentile level, their values diverge a little at higher percentile ranks.

Teleconnections Associated with Strong Winds in Cleveland

As described in the Methods section, strong winds are defined as the top four percentile of daily maximum winds for a given season, over all years. Table 4 shows the years with the greatest and smallest numbers of strong wind days. Figure 6 shows the 700 hPa geopotential height patterns associated with the difference between these high and low years. Table 5 gives the geographic coordinates used to define custom indices of 700 hPa height and R^2 values of these indices' correlation to strong wind events, and Figure 7 shows scatterplots and regression lines of indices and strong wind events for each season.

The pattern indicating more strong wind events during DJF (Fig. 6a) has a high center in the North Sea that does not reach the 95% significance level, and multiple low centers—north of Russia, west of the Straits of Gibraltar, and over north central North America. In formulating the index, preference was given to the low center over North America, which is statistically significant. The regression (Fig. 7a) gives a relatively large R^2 of 0.191.

The MAM pattern (Fig. 6b) is similar to the DJF pattern (Fig. 6a) with its centers shifted north and east. The dipole between northern Scandinavia and the Hudson Bay area yields a regression with R^2 of 0.141 (Fig. 7b). The greatest magnitude part of the negative center near Hudson Bay is not statistically significant, but an area farther northwest is. The strong wind events during MAM are spread more evenly among the years than during DJF. Thus, while the maximum number of strong wind events during DJF in one year was 14, during MAM it was 11. This more even spread also leads to a shallower slope of the regression line in Figure 7b compared to Figure 7a, and hence requires a stronger shift in the index to predict a change in strong wind events.

TABLE 4. Years with high and low number of strong wind events at Cleveland Hopkins airport during each season (strong wind events are defined in the Methods section). The threshold number of strong wind events required to be in each category is indicated in parentheses.

Season	Years with high number (minimum)	Years with low number (maximum)
December, January, February	1971, 1972, 1975, 1976, 1978, 1981, 1982, 1985, 1988, 1996 (9)	1955, 1957, 1970, 1987, 1995, 1999, 2002, 2003 (1)
March, April, May	1959, 1974, 1976, 1979, 1980, 1981, 1982, 1983, 1985, 1991, 1996 (6)	1952, 1953, 1958, 1967, 1968, 1992, 1998, 1999, 2000, 2001, 2003 (1)
June, July, August	1957, 1958, 1960, 1963, 1964, 1970, 1977, 1980, 1981, 1983, 1984, 1988 (6)	1951, 1954, 1965, 1966, 1967, 1989, 1996, 1997, 2001, 2003 (1)
September, October, November	1957, 1979, 1980, 1981, 1983, 1988, 1990, 1991, 1993 (7)	1951, 1953, 1967, 1968, 1969, 1976 (1)

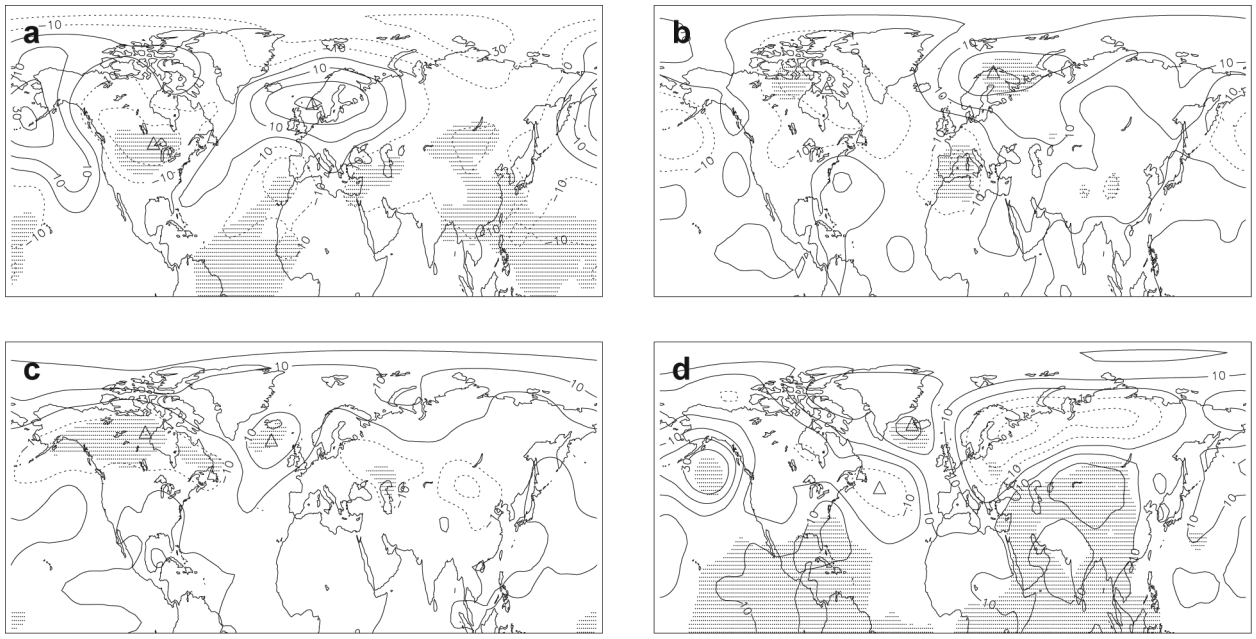

FIG. 6. Difference in 700 hPa height (m) between the years with high numbers of strong wind events and those with low numbers of strong wind events at Cleveland Hopkins airport (high years minus low years) during the seasons of (a) December, January, and February; (b) March, April, and May; (c) June, July, and August; and (d) September, October, and November. The shaded regions indicate statistical significance at the 95% level by a two-tailed Student's t-test. The years used for each of these seasons are given in Table 4. Triangles indicate the positive and negative centers of the custom indices defined in Table 5.

During JJA, more strong wind events are associated with a high center almost directly over Iceland, and a more diffuse low center over northern North America (Fig. 6c). This dipole, with 95% significance at both centers, yields a regression (Fig. 7c) with R^2=0.132. It should be noted that strong winds during the summer are more often associated with thunderstorm activity, which, although often associated with cyclones and fronts, has a more random and short-lived character than the steady winds directly caused by cyclones.

During SON, more strong wind events are again associated with a high center near Iceland, although there is also a high of similar magnitude just south of Alaska. Even though there is a stronger low center over northern Europe, the one closer to North America, over the western Atlantic, was chosen in defining the custom index. The choice of this weaker center may be part of the reason behind the

TABLE 5. Coordinates used in calculation of custom teleconnection indices for strong wind events in Cleveland during each season, as well as R^2 values for the regressions shown in Figure 5. Indices are calculated by taking the geopotential heights at the coordinates labeled "positive center" minus those at the negative center, and subtracting the mean value over all years. Bold letters for the coordinates means that the 700 hPa geopotential height anomaly at that point, shown in Figure 6, is statistically significant at the 95% level of certainty. These points are indicated by triangles in Figure 6.

Season	Positive center	Negative center	R^2
December, January, February	60° N, 5° E	**47.5° N, 92.5° W**	0.191
March, April, May	**70° N, 25° E**	65° N, 77.5° W	0.141
June, July, August	**60° N, 20° W**	**62.5° N, 97.5° W**	0.132
September, October, November	**65° N, 25° W**	45° N, 45° W	0.037

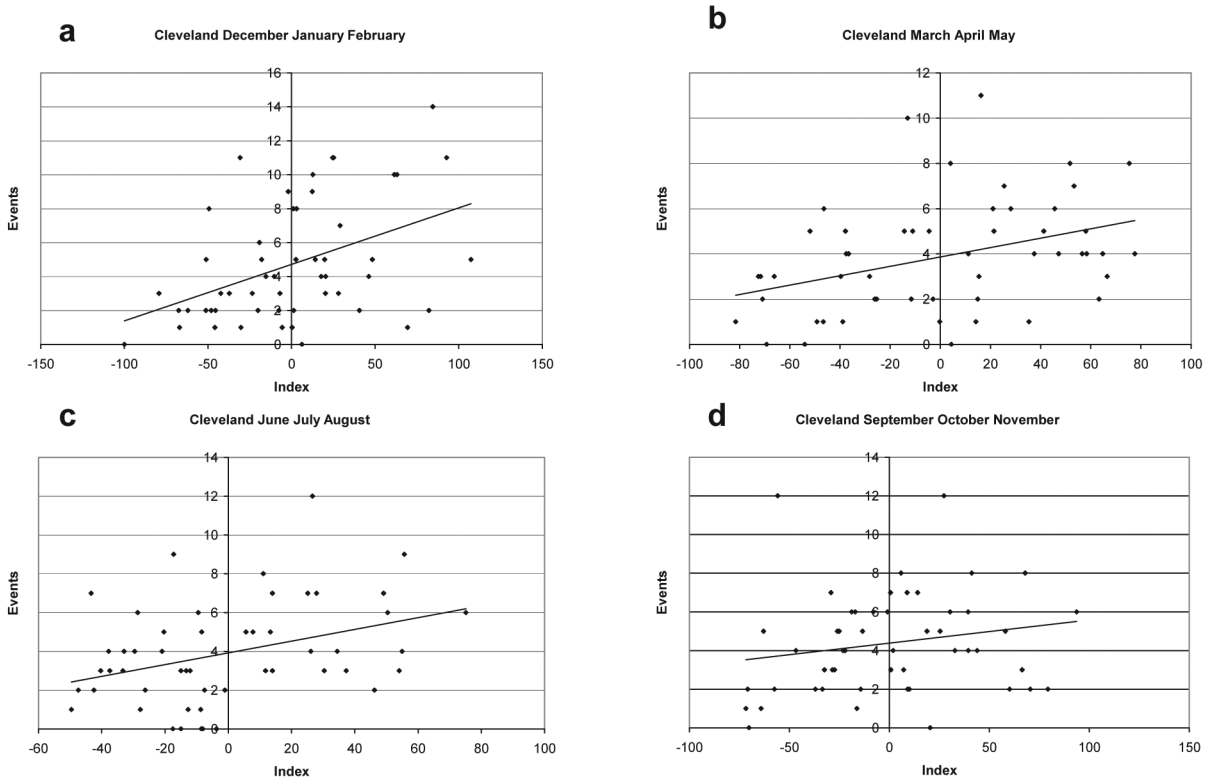

FIG. 7. Scatter plots of number of strong wind events at Cleveland vs. custom indices of 700 hPa height (m) designed to indicate frequency of strong wind events, based on the patterns of 700 hPa height difference shown in Figure 6. Panels are (a) December, January, and February; (b) March, April, and May; (c) June, July, and August; and (d) September, October, and November. The definitions of the indices are shown in Table 5.

smaller R^2 found in this correlation—0.037, which does not achieve the 95% confidence level. The alternate choice of using the low center over Europe (not shown in Table 5) yielded a slightly greater R^2 of 0.047, still not reaching the 95% confidence level.

Resampling of the geopotential height data similar to that described in section 4b, but keyed to the data used in Figure 6 again shows a general agreement of geopotential height patterns between the full sample sets and the subsamples (not shown). Because of the smaller original sample sets (compare Table 4 to Table 1), only 2 or 3 years were eliminated in each subsampled set. The match between the full sampled data and the subsamples was slightly degraded relative to the results of Figure 2, and again the poorest matches were found in the JJA season.

Stronger Cyclones over a Wider Area

As an alternative to simply counting cyclones that pass directly over Lake Erie, we can slightly widen the areal coverage in which we are looking for cyclone passages, but also set a threshold for strength of the cyclones to be considered. This allows for stronger cyclones that are centered nearby but not over Lake Erie to exert an influence on the winds over the lake. The associated teleconnection patterns may possibly agree more closely with those for frequency of strong winds than do the teleconnection patterns associated with any cyclone over the lake.

The region of examination was widened to one bounded by the longitudes of 76.25° and 86.25° W and latitudes of 38.75° and 46.25° N, with the requirement added that the Laplacian of the low pressure center (sum of second derivatives in each horizontal dimension, giving a measure of strength of the cyclone) be at least 1.5×10^{-4} hPa m^{-2}. The resulting teleconnection pattern for DJF (Fig. 8a) is in closer agreement with the pattern for strong wind frequency shown in Figure 6a than the pattern in Figure 2a is. It displays the large low over North

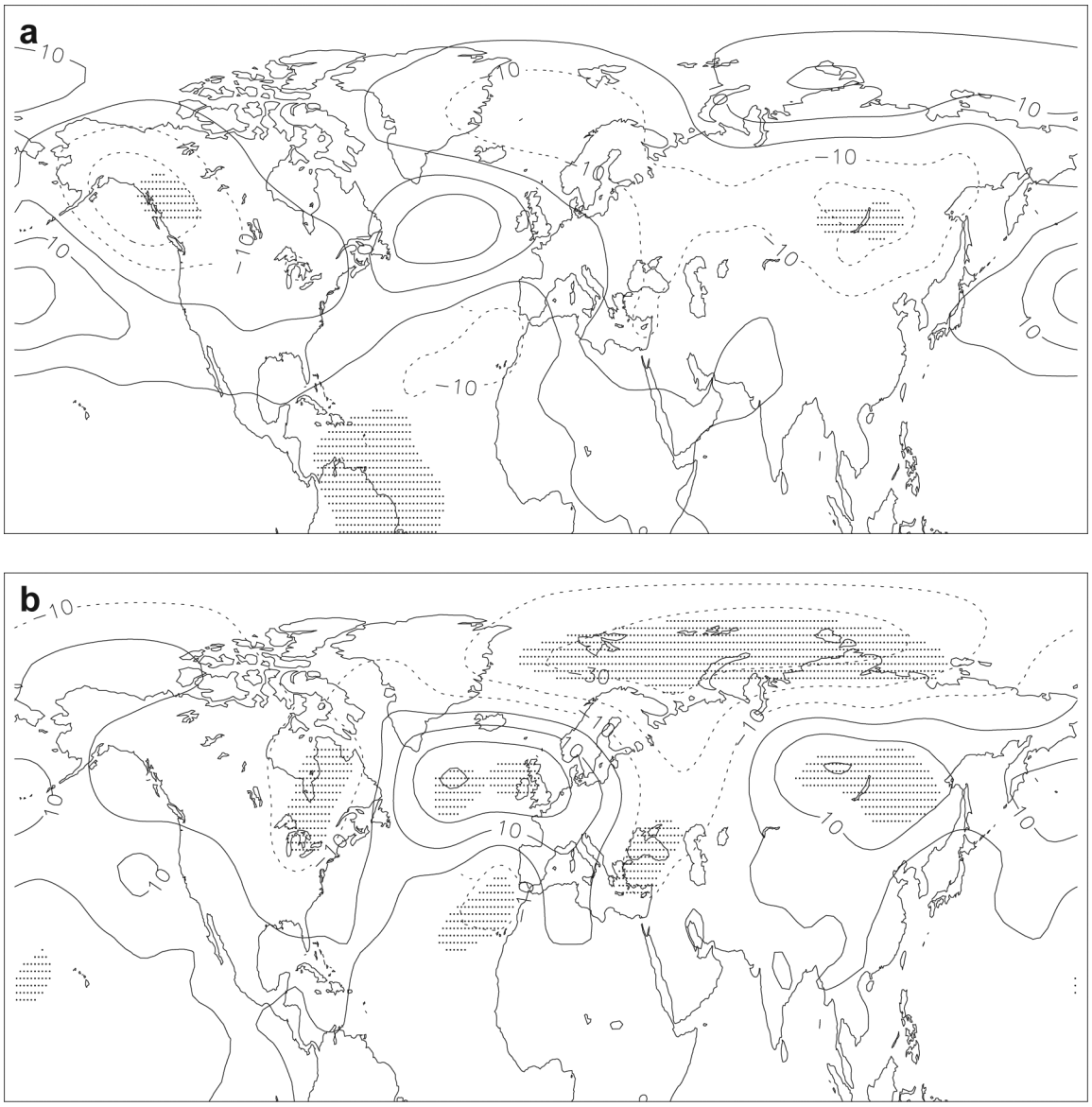

FIG. 8. As in Figure 2, but based on years with cyclone passages through a 7.5° latitude by 10° longitude box surrounding Lake Erie, and restricted to cyclones with a local Laplacian of the sea level pressure field of 1.5×10^{-4} hPa m^{-2}.

America, albeit shifted further west, and the low near northwestern Europe in Figure 6a is also shifted farther west over the Atlantic. Also, the high geopotential height center near the Great Lakes in Figure 2a is replaced by a local minimum in height in Figure 8a, helping to resolve the issue of more low pressure passages through a broad area of higher 700 hPa geopotential height, discussed in the Cyclone Frequency and Teleconnections section.

On the other hand, SON (Fig. 8b) still does not show a strong resemblance to the pattern associated with strong wind events in Figure 6d. Although Figure 8b exhibits some north-south dipole character in the North Atlantic, its location is considerably farther south than in Figure 6d. When combined with the results presented in the Cyclone Frequency and Teleconnections section for all cyclone passages over Lake Erie and compared to the results for teleconnections for strong winds in Cleveland, the commonality between the cyclone and strong wind teleconnections in general could be greater.

DISCUSSION

One thing that is common among several panels of Figures 2 and 6 is that their patterns resemble the negative phase of the North Atlantic Oscillation (NAO), or in several cases, the related Arctic Oscillation (AO). The DJF differences in 700 hPa height based on number of cyclone passages (Fig. 2a) and the SON differences based on number of strong wind events in Cleveland (Fig. 6d) both have features resembling both parts of the negative NAO dipole: a high in the North Atlantic near Iceland and a low in the Atlantic near 40° N. In Figure 2a, however, the high extends across the Arctic region, as in the AO pattern. The DJF (Fig. 6a) and MAM (Fig. 6b) differences based on strong wind events have similar features, but displaced farther east, encroaching onto the European continent. The JJA difference based on strong wind events (Fig. 6c) has only the high anomaly in the North Atlantic.

Serreze *et al.* (1997), in their Figure 8, show that the greater NAO indices of 1983–1993 are associated with more frequent occurrence of cyclones in northeastern North America, although this figure does not depict the Great Lakes region. Their Figure 6, however, shows positive NAO index strongly associated with more cyclones over southeastern Greenland and Iceland, but not over North America.

There is also some commonality in having a low center over northern North America. This is present in the 700 hPa height differences based on cyclone passages for MAM (Fig. 2b) and SON (Fig. 2d), and in the height differences based on strong wind events for all seasons (Fig. 6).

One pattern is evident in the 700 hPa height anomalies during the SON season based on frequency of cyclone passages (Fig. 2d). This has the appearance of a wave train in the west-east direction. Although the centers that are located farther east have greater amplitude than those to the west, the positive center over the North Sea does not reach 95% statistical significance and the predictive value of the other two centers, over central North America and the western Atlantic, are greater (compare Fig. 4d to Fig. 3d). A wave train aligned on more of a great circle orientation is also evident in the DJF season (Fig. 2a), angling to the northeast over the Pacific, then turning toward the east and finally the southeast.

Some aspects of the mechanism by which these custom teleconnections are associated with strong wind events are suggested by Figure 9. These panels show the difference in the magnitude of winds at the 200 hPa level (an estimate of the jet stream) between the 10 years with the greatest values of the custom indices formulated using the points in Table 5 and those with the smallest values. In Figure 9a for DJF, although there is a general decrease in wind magnitude at this level throughout the midlatitudes, this decrease is of lesser magnitude than other midlatitude regions associated with strong jet streams, notably the Atlantic storm track and extending into Europe, and also the Pacific storm track extending toward Alaska.

In Figure 9b for MAM, such a pattern is less identifiable. In general, for years with high MAM indices, 200-hPa winds are greater in swaths in both high-latitude and sub-tropical latitudes. There is a narrow band at mid-latitudes with a decrease, and North America has a departure from this general pattern in the form of a dipole pattern with increased winds over the central United States and decreases farther north. This indicates relative cyclonic horizontal shear at these high levels in the southern Great Lakes region.

During JJA (Fig. 9c), the dipole over the western part of North America between stronger winds to the north and weaker winds to the south is indicative of a northward excursion of the jet in this area. This terminates in enhanced southward winds at this level over eastern North America. Although there may be relative convergence at this level associated with relative deceleration of the jet near the Great Lakes, the beta-effect divergence in geostrophic winds (i.e., arising from a gradient with latitude in the strength of the coriolis force) associated with this may provide a condition promoting the formation of thunderstorms. Such divergence would make this consistent with an association between smaller-scale convective storms and strong winds during the summer, rather than synoptic-scale cyclones. Furthermore, strong winds associated with thunderstorms are likely to be of shorter duration than those associated with cyclones, and thus have less importance in creating deep turbulence in Lake Erie. Unfortunately, summer is one of the primary seasons of interest for such mechanical mixing, because of the tendency for strong thermal stratification and the development of anoxic conditions at depth associated with lack of vertical mixing.

During SON (Fig. 9d), 200 hPa winds are decreased almost everywhere in the Northern Hemisphere in association with the index that is also associated with frequent strong winds in Cleveland.

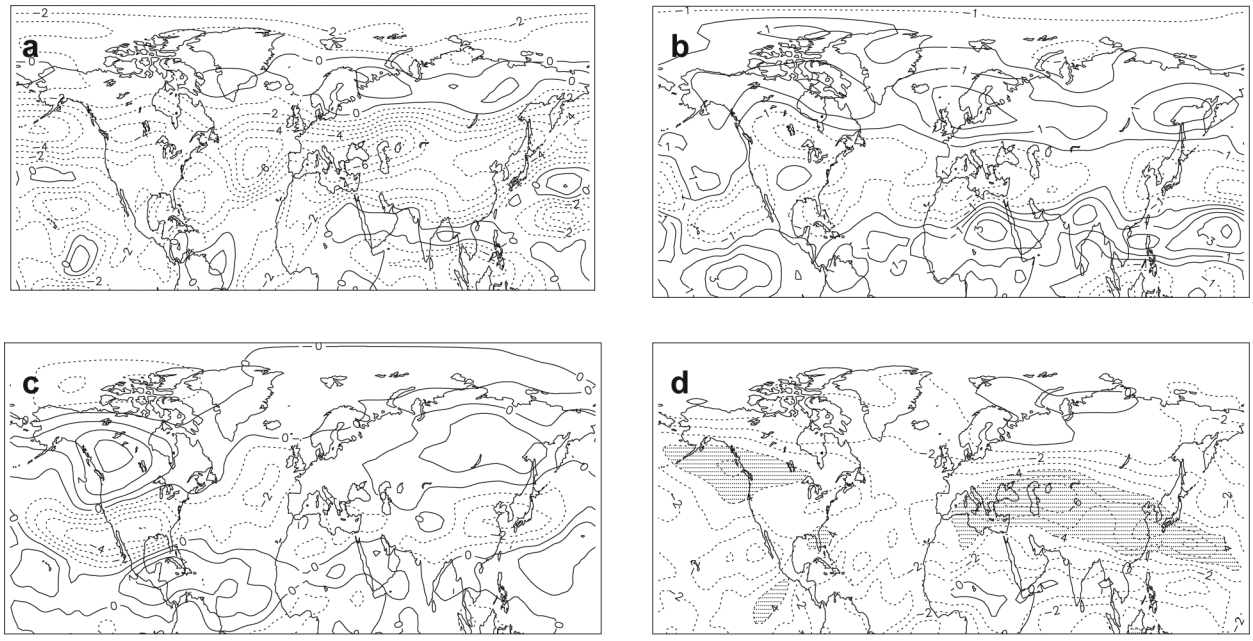

FIG. 9. Difference in mean scalar wind speed (m/s) at 200 hPa between the 10 years with the highest values of the indices defined in Table 5 and the 10 years with the lowest values for (a) December, January, and February, (b) March, April, and May, (c) June, July, and August, and (d) September, October, and November. Dashed contours indicate reductions in the wind speed. In panel (d), values below –4 m/s are shaded in order to emphasize the local maximum decrease over southeastern North America.

However, there is a local maximum in relative wind (i.e., minimum decrease in wind) over and to the southeast of the Great Lakes, which would tend to favor cyclogenesis in this region, although there is a region of greater decrease in winds to the west and northwest, inhibiting the formation of cyclones in this source region.

The definition of custom indices here has some advantages and disadvantages. A primary disadvantage is that the index that was chosen as being associated with the passage of cyclones through Lake Erie does not necessarily correspond to a leading mode of variability in the height field. As a result of this, it is unlikely to be excited by a single coherent mechanism, and its diagnosis and prediction will not be widely studied. Also, as implemented here, there is a degree of subjectivity in selection of points on which to base custom indices, with preference given based on magnitude of the anomaly, statistical significance, and proximity to the area of interest.

On the other hand, the advantage is that this pattern has been identified in a targeted way as being associated with a particular phenomenon of interest. Therefore, if predictive capability can be gained for these custom indices, some skill may be gained in predicting seasonal anomalies in the number of Lake Erie cyclones and strong wind events. Some aid in this is rendered by similarities between these indices and superposition of a few standard teleconnection indices. As noted above, some of these indices bear a resemblance to the negative phase of the NAO, but with shifts in the position of the high and low centers. Thus, combinations of NAO and other standard indices, such as Pacific North America (PNA), may be used to approximate these custom indices.

The fact that the custom indices were chosen by subtracting the years with the smallest number of cyclones or strong wind events from those with the greatest guarantees some level of correlation. Therefore the significance levels, which were assessed as exceeding the 95% level for all but DJF for the cyclone passages (using the index based on the dipole over the Atlantic) and SON for strong wind events, may be exaggerated.

One issue with the statistical treatment used here is that both cyclone passage and strong wind events are defined by counts of events. This is in contrast to temperature and seasonal mean precipitation, con-

tinuum value-type variables that are more commonly used as predictands in teleconnection-based probabilistic outlooks. Thus cyclone passages and wind events are discrete numbers and are not normally distributed. While many values lie in the lower end of the range, there are a few high values, and non-linear relations may result. Even though Figure 4c was used as an example of a linear regression with the yields a wide range of numbers of cyclones fitting the linear regression over the range in values of the index, visual inspection also shows that there is a cluster of several points with the greatest numbers of cyclones at high values of the index. Methods other than traditional linear regression may help to enhance the predicted range in future studies. Additionally, choosing a less restricted region of interest may help in getting a larger sample of cyclones and strong wind events at multiple locations.

Although teleconnection indices are empirically based, their full exploitation is aided by understanding of the mechanism by which the pattern measured by the index affects seasonal climate in a given region, or how that pattern is a signature of a process originating elsewhere. This chain of causality is not fully explored here, and might be a goal of future research. However, as alluded by Figure 9, the patterns associated with the custom indices, are causing shifts in the jet stream and its relative strength over North America and the North Atlantic that lead to changes in cyclone tracks and winds. Another possibility takes the cause and effect in the opposite direction: increased cyclone activity over North America might reduce the overall meridional temperature gradient, and as this air is carried over the Atlantic, a dipole in height fields can develop in the lower and mid-troposphere. Because a variety of patterns have been identified here that have some correlation to cyclones and wind events, investigations into causal mechanisms will require thoughtful prioritization and much work.

An alternative method of seasonal prediction of cyclone activity was investigated by Compo and Sardeshmukh (2004). They found that many-member ensembles of seasonal runs of the National Centers for Environmental Prediction (NCEP) Medium-Range Forecast model (MRF9) and of the National Center for Atmospheric Research (NCAR) Community Climate Model (CCM3) produce minima in the expected skill of forecasts of storm tracks in a zonal band across North America that includes the Laurentian Great Lakes region, as indicated by signal-to-noise ratio within the model ensemble. However, G. Compo (2006, personal communication) shows that an ensemble of runs of the Geophysical Fluid Dynamics Laboratory (GFDL) R30 General Circulation Model yields greater predictability in this region. Overall, the range of studies that attempt to correlate cyclone passages with teleconnection indices is limited, and the present study is one of the first to attempt such correlation with wind events.

CONCLUSIONS

Maps were presented on a seasonal basis that showed the difference in 700 hPa height patterns between years with high numbers and low numbers of cyclone passages through Lake Erie, and high and low numbers of strong wind events at Cleveland Hopkins Airport. These show that both cyclones and strong wind events often are associated with patterns resembling the negative phase of the NAO, or with some aspects more closely resembling the AO because of their spread across longitudes.

Custom teleconnection indices were derived from these maps of 700 hPa height differences, and the seasonal means of each of these indices were linearly regressed against the number of cyclones and the number of strong wind events in that season for each year. This procedure led to moderate, but statistically significant, correlation coefficients. This gives some basis for probabilistic prediction of cyclone passages and strong wind events at Lake Erie.

In order to make skillful predictions based on the empirical relations presented here, there must be skillful predictions of the 700 hPa height. This is more often approached through standard teleconnection indices, such as PNA and NAO. Being based on leading large-scale modes of variability in the atmosphere, or in the atmosphere-ocean system, there is often a stronger signal in these indices and sometimes greater predictability. It may be possible to construct linear combinations of standard teleconnection indices in order to approximate the kind of custom indices developed here. Care should also be taken because there is some possibility that in fact a predominance of cyclones in the midlatitudes of North America may be causing the large-scale patterns in 700 hPa height, rather than the other way around. Another approach is the Classification and Regression Tree (CART) approach used in Rodionov and Assel (2000), which conceptualizes the effect of teleconnection patterns in a non-linear way, depicting their effects as step changes in cli-

mate variables and their variability at certain threshold values of teleconnection indices.

ACKNOWLEDGMENTS

Thanks to Ray Assel, Jim Angel, Gil Compo, and Tom Hamill for useful discussions. Thanks to Karsten Shein for help in getting the metadata for the station winds. Thanks to Mark Serreze for assistance with his dataset. Many thanks to three reviewers for constructive comments that led to improvement of this paper subsequent to its initial submission. Some of this work was accomplished during BML's year as a visitor at NOAA's Earth System Research Laboratory in Boulder, CO. This is GLERL Contribution No. 1452.

REFERENCES

Barnston, A.G., and Livezey, R.E. 1987. Classification, seasonality and persistence of low-frequency atmospheric circulation patterns. *Mon. Wea. Rev.* 115:1083–1126.

Blanken, P.D., Rouse, W.R., and Schertzer, W.M. 2003. On the enhancement of evaporation from a large northern lake by the entrainment of warm, dry air. *J. Hydrometeorol*. 4:680–693.

Compo, G.P., and Sardeshmukh, P.D. 2004. Storm track predictability on seasonal and decadal scales. *J. Climate* 17:3701–3719.

Grover, E.K., and Sousounis, P.J. 2002. The influence of large-scale flow on fall precipitation systems in the Great Lakes basin. *J. Climate* 15:1943–1956.

Hawley, N., Johengen, T.H., Rao, Y.R., Ruberg, S.A., Beletsky, D., Ludsin, S.A., Eadie, B.J., Schwab, D.J., Croley, T.E., and Brandt, S.B. 2006. Lake Erie hypoxia prompts Canada-U.S. study. *Eos Trans. AGU* 87:313.

Isard, S.A., Angel, J.R., and VanDyke, G.T. 2000. Zones of origin for Great Lakes cyclones in North America, 1899–1996. *Mon. Wea. Rev*. 128:474–485.

Kalnay, E., and coauthors. 1996. The NCEP/NCAR 40-year Reanalysis Project. *Bull. Amer. Meteorol. Soc.* 77:437–471.

Lam, D.C.L., and Schertzer, W.M. 1987. Lake Erie thermocline model results: Comparison with 1967–1982 data and relation to anoxic occurrences. *J. Great Lakes Res.* 13:757–769.

Peterson, E.W. and Hennessey, J.P., Jr. 1978. On the use of power laws for estimates of wind power potential. *J. Appl. Meteorol*. 17: 390–394.

Rodionov, S.N. 1994. Association between winter precipitation and water level fluctuations in the Great Lakes and atmospheric circulation patterns. *J. Climate* 7: 1693–1706.

_____, and Assel, R.A. 2000. Atmospheric teleconnection patterns and severity of winters in the Laurentian Great Lakes basin. *Atmosphere-Ocean* 38:601–635.

Serreze, M.C., Carse, F., Barry, R.G., and Rogers, J.C. 1997. Icelandic Low cyclone activity: Climatological features, linkages with the NAO, and relationships with recent changes in the Northern Hemisphere circulation. *J. Climate* 10:453–464.

Wallace, J.M., and Gutzler, D.S. 1981. Teleconnections in the geopotential height field during the Northern Hemisphere winter. *Mon. Wea. Rev.* 109:784–812.

Whittaker, L.M., and Horn, L.H. 1984. Northern Hemisphere extratropical cyclone activity for four mid-season months. *J. Climatol*. 4: 297–310.

Submitted: 3 July 2006
Accepted: 5 October 2007
Editorial handling: William M. Schertzer